Structural basis for the catalytic mechanism of ethylenediamine-N,N′-disuccinic acid lyase, a carbon-nitrogen bond-forming enzyme with broad substrate scope

Poddar, Harshwardhan; De Villiers, Jandre; Zhang, Jielin; Puthan Veetil, Vinod; Raj, Hans; Thunnissen, Andy-mark W.h.; Poelarends, Gerrit J.

Published in:
Biochemistry

DOI:
10.1021/acs.biochem.8b00406

Publication date:
2018

Biochemistry

Article

Cite This: Biochemistry 2018, 57, 3752−3763

pubs.acs.org/biochemistry

Structural Basis for the Catalytic Mechanism of Ethylenediamine-*N*,*N*′-disuccinic Acid Lyase, a Carbon−Nitrogen Bond-Forming Enzyme with a Broad Substrate Scope

Harshwardhan Poddar,[†,§] Jandré de Villiers,[†,∥] Jielin Zhang,[†] Vinod Puthan Veetil,[†,⊥] Hans Raj,[†,#] Andy-Mark W. H. Thunnissen,[*,‡] and Gerrit J. Poelarends[*,†]

[†]Department of Chemical and Pharmaceutical Biology, Groningen Research Institute of Pharmacy, University of Groningen, Antonius Deusinglaan 1, 9713 AV Groningen, The Netherlands

[‡]Molecular Enzymology Group, Groningen Biomolecular Sciences and Biotechnology Institute, University of Groningen, Nijenborgh 4, 9747 AG Groningen, The Netherlands

Supporting Information

ABSTRACT: The natural aminocarboxylic acid product ethylenediamine-*N*,*N*′-disuccinic acid [(*S*,*S*)-EDDS] is able to form a stable complex with metal ions, making it an attractive biodegradable alternative for the synthetic metal chelator ethylenediaminetetraacetic acid (EDTA), which is currently used on a large scale in numerous applications. Previous studies have demonstrated that biodegradation of (*S*,*S*)-EDDS may be initiated by an EDDS lyase, converting (*S*,*S*)-EDDS via the intermediate *N*-(2-aminoethyl)aspartic acid (AEAA) into ethylenediamine and two molecules of fumarate. However, current knowledge of this enzyme is limited because of the absence of structural data. Here, we describe the identification and characterization of an EDDS lyase from *Chelativorans* sp. BNC1, which has a broad substrate scope, accepting various mono- and diamines for addition to fumarate. We report crystal structures of the enzyme in an unliganded state and in complex with formate, succinate, fumarate, AEAA, and (*S*,*S*)-EDDS. The structures reveal a tertiary and quaternary fold that is characteristic of the aspartase/fumarase superfamily and support a mechanism that involves general base-catalyzed, sequential two-step deamination of (*S*,*S*)-EDDS. This work broadens our understanding of mechanistic diversity within the aspartase/fumarase superfamily and will aid in the optimization of EDDS lyase for asymmetric synthesis of valuable (metal-chelating) aminocarboxylic acids.

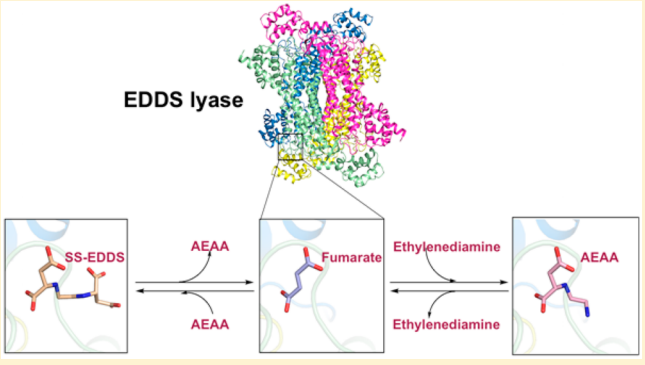

Aminocarboxylic acids that contain several carboxylate groups bound to one or more nitrogen atoms form an important group of metal-chelating agents.[1] The synthetic chelator ethylenediaminetetraacetic acid (EDTA) is a well-known example of this group of metal-complexing compounds. It is used in large amounts in numerous industrial applications, including soil bioremediation and the production of paper, textile, cosmetics, detergents, and fertilizers.[2] Although EDTA is still widely used, there is a growing concern about the adverse environmental effects of this synthetic compound.[2−5] Its high resistance to biodegradation leads to accumulation in the environment. High concentrations of EDTA and its chelating of heavy metals are feared to have a negative effect on drinking water and aquatic life. Hence, aminocarboxylic acid metal chelators that are readily biodegradable are highly desirable as "green" alternatives.

The natural aminocarboxylic acid product ethylenediamine-*N*,*N*′-disuccinic acid [(*S*,*S*)-EDDS], which is produced by a wide range of bacteria to facilitate the uptake of metal ions, is a structural isomer of EDTA.[6,7] Interestingly, (*S*,*S*)-EDDS exhibits chelating properties similar to those of EDTA. However, in contrast to EDTA, (*S*,*S*)-EDDS is readily biodegradable and is therefore an attractive alternative with a favorable environmental profile.[8−10] Previous studies have demonstrated that biodegradation of (*S*,*S*)-EDDS may be initiated by an EDDS lyase, converting (*S*,*S*)-EDDS (**1**) via the intermediate *N*-(2-aminoethyl)aspartic acid (AEAA, **3**) into ethylenediamine (**4**) and two molecules of fumarate (**2**) (Scheme 1).[8−11] Mizunashi first reported the cloning of a gene (from *Brevundimonas* sp. TN3) encoding an EDDS lyase.[11] This *Brevundimonas* enzyme was shown to have potential for use as a biocatalyst in the preparation of EDDS and its derivatives.[11]

Sequence analysis suggested that EDDS lyase belongs to the aspartase/fumarase superfamily.[12] Members of this superfamily include aspartase, fumarase, argininosuccinate lyase, adenylo-

Received: April 9, 2018
Revised: May 9, 2018
Published: May 9, 2018

Scheme 1. Reversible Two-Step Deamination of (*S*,*S*)-EDDS Catalyzed by EDDS Lyase

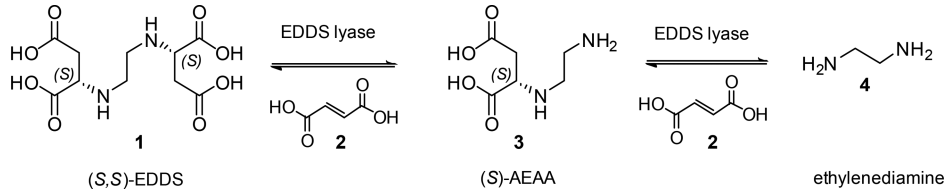

succinate lyase, δ-crystallin, and 3-carboxy-*cis*,*cis*-muconate lactonizing enzyme. They share a common tertiary and quaternary fold, as well as a similar active site architecture, and process succinyl-containing substrates, leading to the formation of fumarate as the common product (except for the CMLE-catalyzed reaction, which results in the formation of a lactone).[12] Current knowledge of the reaction mechanism of EDDS lyase is limited, however, because of the absence of structural data. We have therefore focused our attention on the molecular cloning of an EDDS lyase and initiated structural studies with the aim of elucidating the details of its unusual two-step addition−elimination reaction mechanism.

Here we describe the identification and cloning of the gene encoding EDDS lyase from the bacterium *Chelativorans* sp. BNC1, which was isolated from industrial sewage receiving EDTA-containing wastewater effluents.[13] The enzyme has been purified to homogeneity and subjected to functional and structural characterization. It was found to accept a wide range of structurally distinct amines for addition to fumarate. In addition, we have previously determined that this *Chelativorans* enzyme also accepts a wide variety of amino acids with terminal amino groups for selective amination of fumarate, demonstrating its synthetic usefulness for the production of various important metal-chelating aminocarboxylic acids.[14] Crystal structures of the enzyme in an unliganded state and in complex with formate, succinate, fumarate, AEAA, and (*S*,*S*)-EDDS were determined. These structures confirm a structural fold that is characteristic of the aspartase/fumarase superfamily and support a mechanism that involves general base-catalyzed, sequential two-step deamination of (*S*,*S*)-EDDS.

MATERIALS AND METHODS

Materials. Ingredients for buffers and media were obtained from Duchefa Biochemie (Haarlem, The Netherlands) or Merck (Darmstadt, Germany). All other chemicals used in the experiments, including the sodium salt of (*S*,*S*)-EDDS, fumaric acid, and succinic acid, were purchased from Sigma-Aldrich Chemical Co. (St. Louis, MO) unless stated otherwise. Molecular biology reagents, including restriction enzymes, polymerase chain reaction (PCR) reagents, T4 DNA ligase, and DNA and protein ladders, were obtained from Fermentas (ThermoFisher Scientific, Pittsburgh, PA) or Promega Corp. (Madison, WI). PCR purification, gel extraction, and Miniprep kits were provided by Macherey-Nagel (Duren, Germany). Ni-Sepharose 6 Fast Flow and prepacked PD-10 Sephadex G-25 columns were purchased from GE Healthcare Life Sciences (Uppsala, Sweden). Primers for DNA amplification were synthesized by Eurofins MWG Operon (Cologne, Germany).

General Methods. Techniques for restriction enzyme digestions, ligation, transformation, and other standard molecular biology manipulations were based on standard protocols or as suggested by the manufacturer. PCR was performed in a DNA thermal cycler obtained from Biolegio (Nijmegen, The Netherlands). DNA sequencing was performed by Macrogen (Amsterdam, The Netherlands). Protein was analyzed by polyacrylamide gel electrophoresis (PAGE) under denaturing conditions using sodium dodecyl sulfate (SDS) on precast gels containing 7.5−10% polyacrylamide (Invitrogen). The gels were stained with InstantBlue (Expedeon Inc.). Protein concentrations were determined by the Waddell method.[15] Kinetic data were obtained on a V-650 spectrophotometer obtained from Jasco (IJsselstein, The Netherlands). The kinetic data were fitted by nonlinear regression data analysis using the Grafit program (Erithacus, Software Ltd., Horley, U.K.) obtained from Sigma Chemical Co. Dynamic light scattering (DLS) experiments were performed using a DynaPro MS800TC instrument (Wyatt Technology Corp.) at 20 °C, and data were processed and analyzed with Dynamics software (Wyatt Technology Corp.).

Enzymatic Synthesis of AEAA Using MAL-Q73A. The reference compound *N*-(2-aminoethyl)aspartic acid [(*S*)-AEAA] was synthesized using the previously reported MAL-Q73A enzyme.[16] A solution (80 mL) of fumarate (2 g, 17.24 mmol, 215 mM), 1,2-diaminoethane dihydrochloride (32 g, 240 mmol, 3 M), and $MgCl_2$ (20 mM) was prepared. The pH was adjusted to 9.0 by using aqueous NaOH. The reaction was started by the addition of freshly purified MAL-Q73A enzyme (40 mg, 0.005 mol %), and the reaction mixture was incubated at room temperature. The progress of the reaction was monitored by ultraviolet−visible (UV−vis) spectroscopy. The reaction was stopped after 7 days by incubating the reaction mixture at 100 °C for 10 min, and precipitated protein was removed by filtration. An excess of amine was removed from the reaction mixture by the use of a rotary evaporator. The concentrated crude reaction mixture was dissolved in 50 mL of 1 N HCl, and the desired amino acid product was purified by cation-exchange chromatography by following a previously described protocol.[16] The purified product was obtained as the bis-ammonium salt and identified as *N*-(2-aminoethyl)aspartic acid by ^{1}H nuclear magnetic resonance (NMR) and ^{13}C NMR spectroscopy and HRMS analysis. *N*-(2-Aminoethyl)aspartic acid: conversion 100% (7 days); 61% yield, 2.2 g; brown solid; ^{1}H NMR (500 MHz, D_2O) δ 2.66 (dd, 1H, *J* = 17.3, 9.0 Hz, CHC**H**$_2$), 2.83 (dd, 1H, *J* = 17.3, 3.8 Hz, CHC**H**$_2$), 3.34−3.46 (m, 4H, NHC**H**$_2$C**H**$_2$NH$_2$), 3.83 (dd, 1H, *J* = 9.0, 3.7 Hz, C**H**NH$_2$). ^{1}H NMR signals are in agreement with the literature data.[16]

Cloning of the EDDS Lyase Gene into an Expression Vector. The amino acid sequence of the putative EDDS lyase from *Chelativorans* sp. BNC1, which was annotated as an argininosuccinate lyase, was obtained from the NCBI protein database under GenBank entry ABG61966 (NCBI reference sequence WP_011579909.1). The corresponding DNA sequence was codon-optimized for *Escherichia coli* and synthesized by Eurofins MWG Operon (Ebersberg, Germany). The gene was delivered in the pBSII SK+ vector with restriction sites for *Nde*I and *Hin*dIII at the 5′ and 3′ ends of the gene, respectively. The gene was amplified by PCR using primers

DOI: 10.1021/acs.biochem.8b00406
Biochemistry 2018, 57, 3752−3763

Ed_fw-NdeI (GGAGGAATTA**CATATG**AACATCAACGTACCGGACGC) and Ed_his-st-rv-*Hin*dIII (CAT**AAGCTT**TATCAATGATGATGATGATGGCGCAGATATTTGCGGTCGG) (the restrictions sites are depicted in bold), digested with *Nde*I and *Hin*dIII, and cloned into the pBAD*N*/*Myc*-His A expression vector to obtain the pBADN(EDDS-His) construct. The entire gene was sequenced to verify that no mutations were introduced during the cloning procedure.

Expression and Purification of EDDS Lyase. The His_6-tagged enzyme was overproduced in *E. coli* TOP10 cells using the pBADN(EDDS-His) expression plasmid. Freshly transformed TOP10 cells containing this plasmid were used to inoculate 10 mL of LB/Amp medium. After overnight growth at 37 °C, this culture was used to inoculate 1 L of LB/Amp medium in a 5 L Erlenmeyer flask. Cultures were grown to an A_{600} of 0.4−0.6 at 37 °C while being vigorously shaken, induced with arabinose [0.04% (w/v)], and placed at 20 °C for overnight incubation (∼16 h). Cells were harvested by centrifugation (6000*g* for 15 min) and stored at −20 °C until further use.

In a typical purification experiment, cells from a 1 L culture (∼5.0 g wet weight) were thawed and suspended in 10 mL of lysis buffer [50 mM Tris-HCl and 20 mM imidazole (pH 8.0)]. Cells were disrupted by sonication for 4 × 1 min (with a 5 min rest between each cycle) at a 60 W output, after which unbroken cells and debris were removed by centrifugation (10000*g* for 30 min). The supernatant was filtered through a 0.45 μm-pore diameter filter and incubated with Ni-Sepharose (1 mL slurry in a small column at 4 °C for ≥18 h), which had previously been equilibrated with lysis buffer. The nonbound proteins were eluted from the column by gravity flow. The column was first washed with lysis buffer (10 mL) and then with buffer A [50 mM Tris-HCl and 40 mM imidazole (pH 8.0), 10 mL]. Retained proteins were eluted with buffer B [50 mM Tris-HCl and 500 mM imidazole (pH 8.0), 4 mL]. Fractions were analyzed by SDS−PAGE on gels containing 10% acrylamide; those that contained purified EDDS lyase were pooled, and the buffer was exchanged against 50 mM Tris-HCl (pH 8.0) and 200 mM NaCl using a prepacked PD-10 Sephadex G-25 gel filtration column. The purified enzyme (yield of ∼50 mg) was stored at 4 or −20 °C until further use.

Construction and Production of EDDS Lyase Mutants. The S280A and D290A mutants of EDDS lyase were constructed using the QuikChange site-directed mutagenesis method (Stratagene). Plasmid pBADN(EDDS-His) was used as a template. For the S280A mutation, the following oligonucleotides were used as forward and reverse primers: 5′-GCGGGAACC**GCG**TCGATCATGCCGC-3′ and 5′-GCGGCATGATCGA**CGC**GGTTCCCGC-3′, respectively (the mutated codon is depicted in bold). For the D290A mutation, the following oligonucleotides were used as forward and reverse primers: 5′-CGCAGAAGAAGAACCCG**GCT**AGCCTGGAACGTAGTCGC-3′ and 5′-GCGACTACGTTCCAGGCT**AGC**CGGGTTCTTCTTCTGCG-3′, respectively (the mutated codon is depicted in bold). DNA sequencing of the mutant genes was performed to ensure that only the desired mutation had been introduced.

The S280A and D290A mutants were produced and purified using protocols similar to those used for wild-type EDDS lyase. The S280A mutant was further purified by gel filtration chromatography with a Superdex 200 10/300 GL column (GE Healthcare) using 0.1 M NaCl in 50 mM Tris-HCl buffer (pH 7.5) as an eluent, whereas the D290A mutant was further purified to homogeneity by gel filtration chromatography with a HiLoad 16/600 Superdex 200 pg column (GE Healthcare) using 20 mM NaH_2PO_4 buffer (pH 8.5) as an eluent. Activity assays were performed with freshly purified proteins (notably, some protein precipitation was observed upon storage of the S280A mutant, indicative of poor stability).

Enzyme Assays. Kinetic assays were performed at 25 °C in 50 mM Tris-HCl buffer (pH 8.0), revealing the increase in absorbance at 240 nm corresponding to the formation of fumarate (ε = 2530 M^{-1} cm^{-1}). An aliquot of EDDS lyase (180 μg) was diluted into buffer (15 mL) and incubated for 30 min at 25 °C. Subsequently, a 1 mL portion was transferred to a 10 mm quartz cuvette, and the enzyme activity was assayed by the addition of a small quantity (0.5−20 μL) of (*S*,*S*)-EDDS from a stock solution (10 mM). The stock solution was made up in 50 mM Tris-HCl buffer (pH 8.0). The concentrations of (*S*,*S*)-EDDS used in the assay ranged from 0.005 to 0.2 mM.

The pH optimum of EDDS lyase was determined in 50 mM phosphate buffers with pH values ranging from 4.4 to 9.2 at 25 °C. A sufficient quantity of enzyme was added (12 μg/mL) and its activity assayed by adding (*S*,*S*)-EDDS from a stock solution to a final concentration of 0.1 mM, following the increase in absorbance at 240 nm corresponding to the formation of fumarate. The initial reaction rates were plotted against pH.

The temperature optimum was determined in Tris-HCl buffer (50 mM, pH 8.0), using a temperature range of 10−80 °C. At each temperature, the pH of the Tris buffer was adjusted to the desired value of 8.0. A 1 mL portion of the buffer was transferred to a 10 mm cuvette; a sufficient quantity of enzyme was added (12 μg/mL), and its activity was assayed using 0.1 mM (*S*,*S*)-EDDS (2 μL of a 50 mM stock solution) as the substrate. Substrate stock solutions were made in Tris-HCl buffer (50 mM, pH adjusted to 8.0). The initial reaction rates were plotted against temperature.

Enzymatic Synthesis of AEAA and (*S*,*S*)-EDDS Using EDDS Lyase. A reaction mixture containing fumaric acid (50 mM) and ethylenediamine (10 mM) was prepared in 20 mM NaH_2PO_4-NaOH buffer (pH 8.5). EDDS lyase (14 mg, 0.05 mol %) was added to start the reaction, and the reaction volume was immediately adjusted to 50 mL with 20 mM NaH_2PO_4-NaOH buffer (pH 8.5). The reaction was allowed to proceed at room temperature. At different time points, reaction samples (0.5 mL) were taken from the reaction mixture and boiled for 10 min to inactivate the enzyme. The samples were dried under vacuum and redissolved in 0.5 mL of D_2O for ^1H NMR measurements.

The ^1H NMR (500 MHz, deuterium oxide) signals of (*S*,*S*)-EDDS are δ 3.57 (dd, *J* = 8.7, 4.3 Hz, 2H), 3.08−2.88 (m, 4H), 2.66 (dd, *J* = 16.2, 4.3 Hz, 2H), 2.48 (dd, *J* = 16.2, 8.8 Hz, 2H). The ^1H NMR signals (500 MHz, deuterium oxide) of AEAA are δ 3.43 (dd, *J* = 10.4, 3.7 Hz, 1H), 3.14−2.92 (m, 3H), 2.84−2.77 (m, 1H), 2.60 (dd, *J* = 15.5, 3.7 Hz, 1H), 2.29 (dd, *J* = 15.5, 10.4 Hz, 1H). After 24 h, the ratio between AEAA and (*S*,*S*)-EDDS in the reaction mixture was ∼2:1, calculated by integration of the signals at 3.43 and 3.57 ppm, respectively.

Substrate Scope and Product Identification by Liquid Chromatography−Tandem Mass Spectrometry (LC−MS/MS). Various amines were tested as substrates for EDDS lyase in the addition to fumarate. Fumarate (5 mM), amine (400 mM), and EDDS lyase (0.5 mg/mL, 0.17 mol %) in 50 mM Tris-HCl buffer (pH 8.0) were incubated at room temperature in a 96-well plate (final volume of 150 μL). Reactions were monitored by UV spectroscopy, following the

DOI: 10.1021/acs.biochem.8b00406
Biochemistry 2018, 57, 3752−3763

decrease in absorbance at 240 nm corresponding to the depletion of fumarate.

For several selected amine substrates, reactions were performed with two different substrate ratios and the products identified via LC−MS/MS. Reactions were initially performed with a 20-fold excess of amine. Fumarate (50 mM), amine (1000 mM), and EDDS lyase (0.5 mg/mL) in buffer [Tris-HCl (pH 8.0)] were incubated for 24 h. Reactions were subsequently also performed with a 2-fold excess of fumarate. Fumarate (100 mM), amine (50 mM), and EDDS lyase (0.1 mg/mL) in buffer [Tris-HCl (pH 8.0)] were incubated for 24 h. All samples were prepared for LC−MS/MS analysis as follows. After incubation of the reaction mixture for 24 h, the samples were incubated at 100 °C for 1−2 min to stop the reaction. The precipitated enzyme was removed by centrifugation. The supernatant was filtered (0.42 μm filter) and subjected to LC−MS/MS to confirm formation of single- and/or double-addition products. Mass spectrometric analysis was performed by the Mass Spectrometry Facility Core in the Department of Pharmacy at the University of Groningen.

Crystallization. Before crystallization trials were set up, the EDDS lyase protein sample was further purified by gel filtration chromatography with a Superdex 200 (GE Healthcare) column using 0.2 M NaCl in 50 mM Tris-HCl buffer (pH 7.5) as an eluent. The protein eluted as a tetramer with an apparent molecular weight of ∼200 kDa, as confirmed by dynamic light scattering analysis. The protein sample was concentrated to 9 mg/mL using a centrifugal concentrator (Vivaspin 15R, 30 kDa molecular weight cutoff, Sartorius Stedim Biotech). A search for crystallization conditions was performed using various commercial crystallization screens. Screening was performed at room temperature in 96-well sitting-drop crystallization plates using a robot (Mosquito, TTP LabTech) to dispense 300 nL drops (1:1 protein:reservoir ratio). A single cube-shaped crystal was obtained directly from the Structure Screen (Molecular Dimensions) with a solution containing 0.1 M HEPES (pH 7.5) and 4 M NaCl, but this condition could not be reproduced. Crystals also grew at a condition from Clear Strategy Screen II (Molecular Dimensions), containing 0.1 M sodium cacodylate (pH 6.5) and 2.0 M sodium formate. Small crystals would typically appear within 1 h of the crystallization plates being set up, reaching a maximum size of approximately 140 μm × 90 μm × 80 μm after overnight growth.

Crystal soaking experiments for trapping a substrate, intermediate, or product in the active site of EDDS lyase were unsuccessful, probably because of the high sodium formate concentration in the crystallization solution and the presence of bound formate ions in the active site. Thus, an alternative strategy was employed, replacing sodium formate in the crystallization condition by sodium salts of fumaric acid, succinic acid, (*S*,*S*)-EDDS, or a bis-ammonium salt of AEAA (synthesized as described above). Diffracting crystals appeared overnight, with all of the salts mentioned above at a concentration of 0.2−0.3 M, like the crystals grown in the presence of sodium formate. As an additional strategy for trapping an intermediate-bound state of EDDS lyase, crystals co-crystallized with fumarate were soaked for 30 s in drops of mother liquor [0.1 M sodium cacodylate (pH 6.5) and 0.3 M fumarate] containing 20 mM ethylenediamine or AEAA, immediately followed by flash cooling in liquid nitrogen.

X-ray Data Collection and Crystal Structure Determination. Prior to X-ray data collection, crystals were briefly transferred to drops containing mother liquor supplied with 25% PEG 400 and flash-cooled in liquid nitrogen. All the diffraction data were collected in house at 110 K using a Microstar rotating Cu anode X-ray source (Bruker AXS GmbH) in combination with Helios optics (Incoatec GmbH) and a MAR345dtb detector (MarResearch GmbH). Data sets were integrated and scaled using XDS[17] and merged using the program AIMLESS[18] from the CCP4 software suite.[19] All crystals belonged to the *F*222 space group and contained a single polypeptide chain per asymmetric unit, with a solvent content of ∼62%. Relevant data collection and refinement statistics are listed in Table S2. The upper resolution limit of the data sets varied between 2.6 and 1.9 Å. It should be noted that some of the data sets were recorded with a non-optimal crystal-to-detector distance, in which cases the actual resolution limit of the diffraction was somewhat higher. Structure determination was started with diffraction data collected from the single crystal obtained at 4 M NaCl. The program PHASER[20] from the CCP4 package was used to obtain initial phases by molecular replacement. With the help of the Fold and Function Assignment Server (FFAS),[21] an ensemble of three homologous protein structures was used as a molecular replacement search model: duck δ-crystallin II [28% identity, Protein Data Bank (PDB) entry 1TJU],[22] argininosuccinate lyase from *Thermus thermophilus* HB8 (30% identity, not published, PDB entry 2E9F), and duck δ-crystallin I (29% identity, PDB entry 1U15).[23] Automatic model building was performed using ARP/wARP.[24] The programs REFMAC5[25] and COOT[26] were used for subsequent rounds of refinement and model building, including the placement and validation of water molecules. The final rounds of refinement were performed using phenix.refine from the Phenix software suite.[27] All other structures were adapted and refined starting from the apo structure, using identical strategies and software. Coordinates and restraints for formate, fumarate, and succinate were readily available from the CCP4 database with the following ligand identifiers, FMT, FUM, and SIN. Coordinates and restraints for (*S*,*S*)-EDDS and AEAA were generated using the PRODRG2 server[28](ENSUCP, CCDC no. 1149819)

Crystal Structure Analysis. Molprobity[29] was used for validating the stereochemical quality of the models. Structure-based sequence alignments were performed using T-coffee[30] and visualized using the ESPript 3.0 server.[31] Superpositions and calculation of Cα backbone root-mean-square deviation (rmsd) values were performed using the protein structure comparison service Fold at the European Bioinformatics Institute.[32] PyMOL (Schrödinger)[33] was used for structure analysis and figure preparations. ChemBioDraw 12.0 was used to draw schemes and chemical structures. Atomic coordinates and structure factors have been deposited in the PDB (www.rcsb.org) as entries 6G3D, 6G3E, 6G3F, 6G3G, 6G3H, and 6G3I.

RESULTS

Identification of an EDDS Lyase in *Chelativorans* sp. BNC1. A sequence similarity search in the NCBI microbial database was performed with the BLASTP program using the EDDS lyase amino acid sequence from *Brevundimonas* sp. TN3 as the query. This search yielded several bacterial proteins that had sequences significantly similar to that of EDDS lyase. The top hits included a sequence from the bacterium *Chelativorans* sp. BNC1, which was isolated from industrial sewage receiving EDTA-containing wastewater effluents.[13] This *Chelativorans* protein, with a sequence that is 79% identical to that of EDDS

DOI: 10.1021/acs.biochem.8b00406
Biochemistry 2018, 57, 3752−3763

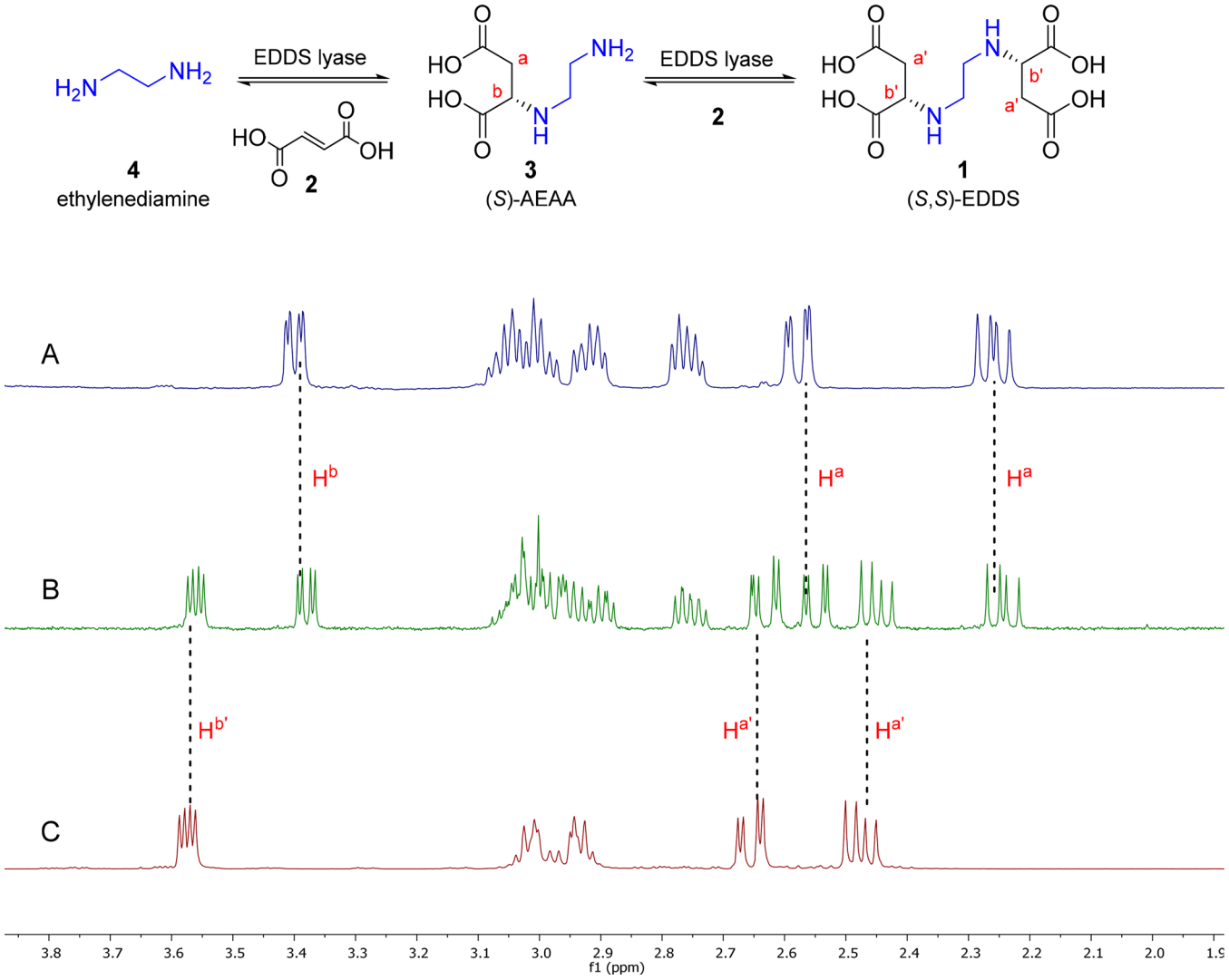

Figure 1. EDDS lyase-catalyzed addition of ethylenediamine (**4**) to fumaric acid (**2**) yielding AEAA (**3**) and EDDS (**1**). (A) ^{1}H NMR spectrum of AEAA (**3**) in D_2O. (B) ^{1}H NMR spectrum of the reaction mixture after incubation for 24 h. The reaction was started by addition of EDDS lyase (0.05 mol %) to fumaric acid (50 mM) and ethylenediamine (10 mM) in 20 mM NaH_2PO_4-NaOH buffer (pH 8.5). (C) ^{1}H NMR spectrum of (*S*,*S*)-EDDS (**1**) in D_2O. The assignments of key signals are highlighted in red.

lyase from *Brevundimonas* sp. TN3 (Figure S1),[11] was annotated as a putative argininosuccinate lyase and selected for further study.

The gene encoding the EDDS lyase homologue from *Chelativorans* sp. BNC1 was cloned into expression vector pBADN/*Myc*-His A, resulting in the construct pBADN(EDDS-His). Using this expression plasmid, the enzyme was produced upon induction with arabinose in *E. coli* TOP10 as a C-terminal hexahistidine fusion protein. The enzyme was purified by a one-step Ni-Sepharose affinity chromatography protocol, which typically provides ~30 mg of homogeneous enzyme per liter of culture. Analysis of the purified enzyme by size-exclusion chromatography and dynamic light scattering revealed a native molecular mass of ~200 kDa. A comparison of this value to that of the calculated subunit mass suggests that the enzyme is a homotetrameric protein.

To examine whether the *Chelativorans* enzyme can promote the synthesis of AEAA (**3**) and EDDS (**1**), the enzyme was incubated with fumarate (**2**) and ethylenediamine (**4**) and the reaction was monitored by ^{1}H NMR spectroscopy (Figure 1). The results showed that the enzyme indeed catalyzes the addition of ethylenediamine to fumarate to give AEAA and (*S*,*S*)-EDDS. The enzyme also catalyzes the reverse reaction, that is, the deamination of (*S*,*S*)-EDDS to yield AEAA, fumarate, and ethylenediamine, as determined by UV and ^{1}H NMR spectroscopy (data not shown). Having established that the *Chelativorans* enzyme exhibits EDDS lyase activity, we determined kinetic parameters (at 25 °C) and the optimum pH and temperature. The enzyme catalyzes the deamination of (*S*,*S*)-EDDS with a k_{cat} of 6.5 ± 0.2 s^{-1} and a K_m of 16 ± 3 μM and shows maximum activity at pH 8.0 and 60 °C (Figure S2). Notably, incubation of the enzyme with fumarate and arginine showed that the enzyme displays no argininosuccinate lyase activity.

Substrate Scope of EDDS Lyase. It has previously been determined that the *Chelativorans* enzyme accepts a wide variety of amino acids with terminal amino groups for selective addition to fumarate, yielding the natural products Aspergillomarasmine A and Aspergillomarasmine B, as well as various related aminocarboxylic acids (Scheme S1).[14] To further explore the substrate scope of EDDS lyase, the enzyme was incubated with fumarate and different amines and the rate of

DOI: 10.1021/acs.biochem.8b00406
Biochemistry 2018, 57, 3752−3763

the reactions was monitored spectrophotometrically by following the depletion of fumarate at 240 nm. The results showed that EDDS lyase has a broad nucleophile scope and accepts various mono- and diamines as unnatural substrates in the amination of fumarate, albeit with a catalytic efficiency lower than that of the reaction with the native substrate ethylenediamine (Table 1). For several selected substrates, the enzymatic addition reactions were performed with either a 20-fold excess of amine or a 2-fold excess of fumarate, and formation of the corresponding single- and double-addition products was assessed by LC−MS/MS (Table S1). The results

Table 1. Relative Activities of EDDS Lyase toward Ammonia and Various Amines

Entry	Substrate	Substrate Structure	Relative Activity [%]
1	**4a**	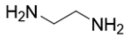	100[a]
2	**4b**		2
3	**4c**		< 1
4	**4d**		< 1
5	**4e**	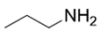	< 1
6	**4f**	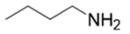	< 1
7	**4g**	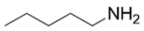	6
8	**4h**		3
9	**4i**		9
10	**4j**	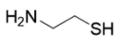	6
11	**4k**	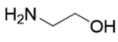	34
12	**4l**	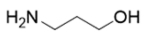	14
13	**4m**	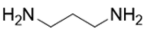	59
14	**4n**	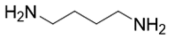	< 1
15	**4o**	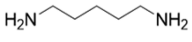	< 1
16	**4p**	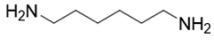	1
17	**4q**	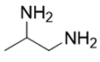	112
18	**4r**	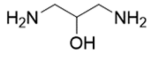	74
19	**4s**	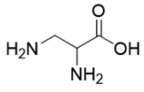	23
20	**4t**	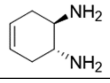	2

[a]The initial rate of the enzyme-catalyzed addition of ethylenediamine to fumarate was assigned as 100% activity.

demonstrate that by using an appropriate molar ratio of starting substrates, different aminocarboxylic acid products, including EDDS derivatives, can be prepared using EDDS lyase as the catalyst. In contrast to its very broad nucleophile scope, the enzyme was found to be highly specific for fumarate, with fumaric acid monomethyl ester, crotonic acid, mesaconic acid, itaconic acid, 2-pentenoic acid, and glutaconic acid not accepted as alternative electrophiles.

Overall Structure of EDDS Lyase. The crystal structure of EDDS lyase was determined at 2.2 Å resolution by molecular replacement and refined to a crystallographic *R*-factor of 18.2% (R_{free} = 22.2%) with good geometry (Table S2). Diffraction data were obtained from a single crystal grown in the presence of 4 M NaCl at pH 7.5. The EDDS lyase crystal structure belongs to space group *F*222 and contains one monomer per asymmetric unit (labeled A): the other three subunits (B−D) of the functional tetramer are "generated" by crystallographic 2-fold axes. The final model consists of 496 residues; only the first five residues at the N-terminus and the last seven residues at the C-terminus, which comprises Arg502 and the $(His)_6$ tag, could not be modeled because of weak or absent electron density.

The overall fold and topology of EDDS lyase closely resemble those of other members of the aspartase/fumarase superfamily (Figures 2 and 3).[12] The dumbbell-shaped, mainly α-helical subunit can be subdivided into three domains (Figure 2a): an N-terminal domain (residues 6−111), an elongated central domain (residues 112−351), and a C-terminal domain (residues 352−501). In the functional tetramer (Figure 2b), the central domains of the four subunits interact coaxially to form a tightly packed bundle of 20 α-helices, with the N- and C-terminal domains of neighboring subunits positioned near each other at the ends. Each active site (there are four in the tetramer) is composed of three regions of highly conserved amino acid residues, each of which originates from a different subunit (Figure S3 and Figure 2b). These conserved regions are C1 (residues 111−114; for a representative active site we will refer to the subunit as A), C2 (residues 158−165, subunit B), and C3 (also known as the "SS loop", residues 279−293, subunit C).[12]

Two striking differences are observed between the overall structure of EDDS lyase and those of other aspartase/fumarase superfamily members (Figure 3). First, the EDDS lyase subunit contains a final C-terminal α-helix (residues 451−500) that is elongated (Figure S3) and runs alongside the entire length of the central domain back to the N-terminal domain. Second, within a subunit, the first ~30 residues at the N-terminus form a loop (residues 5−15) and a short α-helix (residues 20−31), which fold away from the N-terminal domain to pack against the central domain and SS loop. Two arginine residues (Arg10 and Arg13) in the N-terminal loop form hydrogen bonds with the main chain carbonyls of Ala274, Ala277, and Gln285, effectively locking the SS loop in place. In the tetramer, each SS loop is further stabilized by interactions with residues of the N- and C-terminal domains from two neighboring subunits, resulting in a rigid and well-defined conformation. In the structures of other aspartase/fumarase superfamily members, the SS loop is intrinsically flexible and can undergo an open−closed transition upon binding of substrate.[12,34−37] In EDDS lyase, the occurrence of such a transition of the SS loop is unlikely: the additional interactions with the N-terminal loop region stabilize a conformation that is highly similar to the catalytically competent closed conformation observed in the

DOI: 10.1021/acs.biochem.8b00406
Biochemistry 2018, 57, 3752−3763

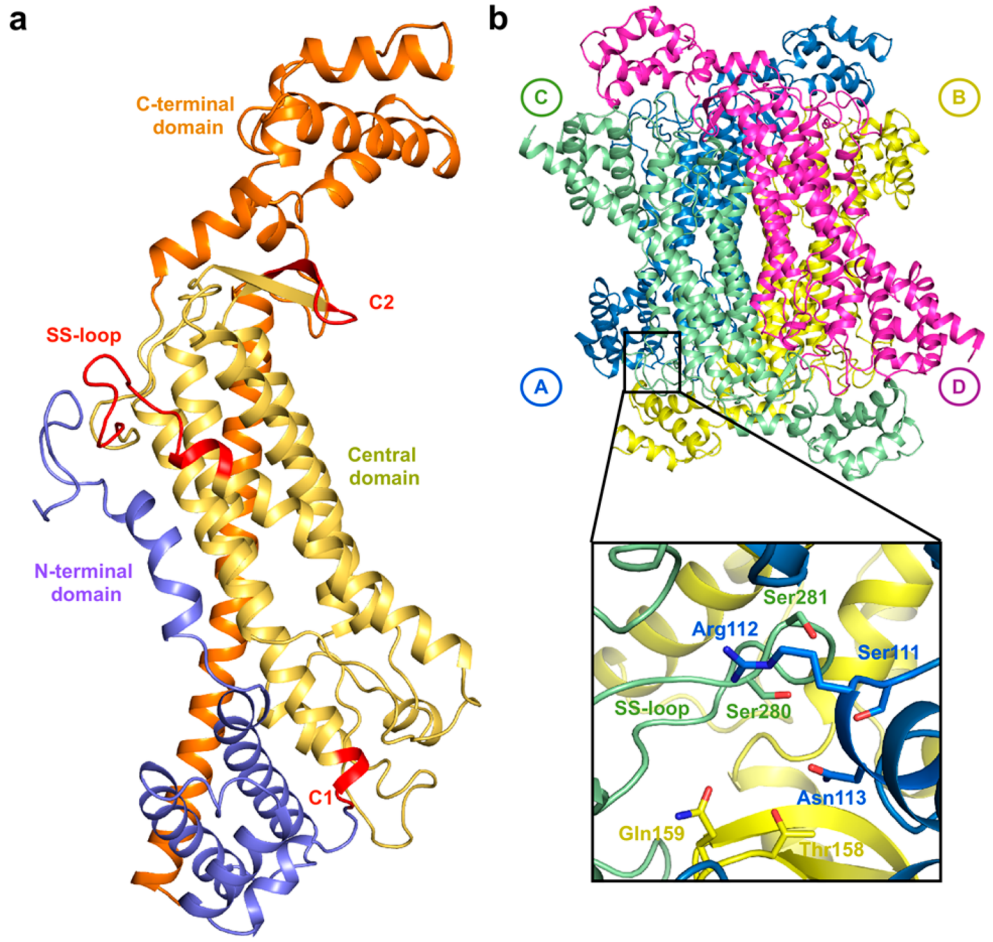

Figure 2. Overall structure of EDDS lyase. (a) Cartoon representation of a monomer. The N-terminal domain, central domain, and C-terminal domain are colored blue, yellow, and orange, respectively. The conserved regions C1, C2, and SS loop are colored red. (b) Cartoon representation of the functional tetramer, with the polypeptide chains in different colors. The inset shows a close-up of an active site (viewing orientation different from that for the tetramer). Residues from the conserved regions forming the composite active site are shown as sticks.

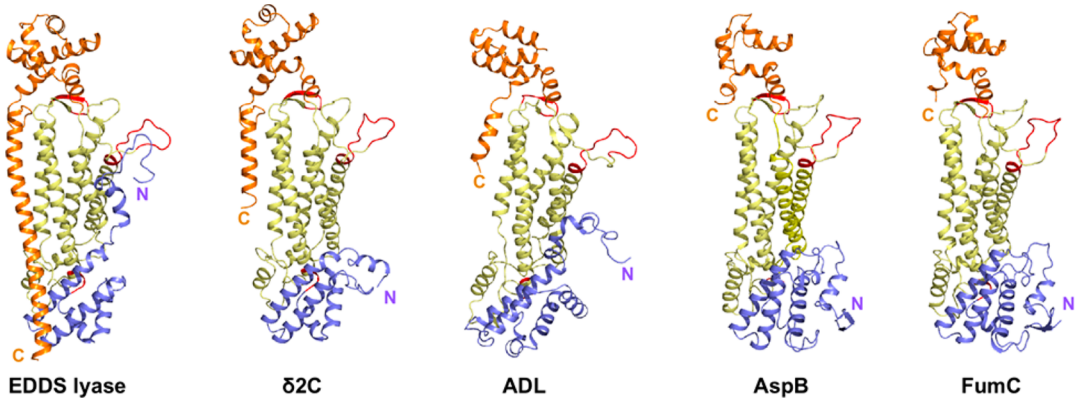

Figure 3. Comparison of the EDDS lyase monomer with other aspartase/fumarase superfamily enzymes. Cartoon representation of apo EDDS lyase (PDB entry 6G3D), argininosuccinate lyase (*δ*2C, PDB entry 1HY1), adenylosuccinate lyase (ADL, PDB entry 2PTR), aspartase (AspB, PDB entry 3R6V), and fumarase (FumC, PDB entry 1YFE). The N-terminal domain, central domain, and C-terminal domain are colored blue, yellow, and orange, respectively. The conserved regions C1, C2, and SS loop are colored red. The locations of the N- and C-termini are also shown.

structures of other aspartase/fumarase superfamily members, even when no substrate is bound.

Formate-, Fumarate-, and Succinate-Bound Structures. During the initial crystallization screening, a condition that included 2.0 M sodium formate (pH 6.5) also yielded protein crystals. The crystals belonged to the same space group, *F*222, obtained with 4 M NaCl, with identical cell parameters, and allowed a structure determination at 1.9 Å resolution. The overall structure of EDDS lyase in the crystals grown with sodium formate is identical to that of the crystal obtained with sodium chloride, including the conformation of the SS loop (the structures superpose with an rmsd value of only 0.26 Å).

DOI: 10.1021/acs.biochem.8b00406
Biochemistry 2018, 57, 3752−3763

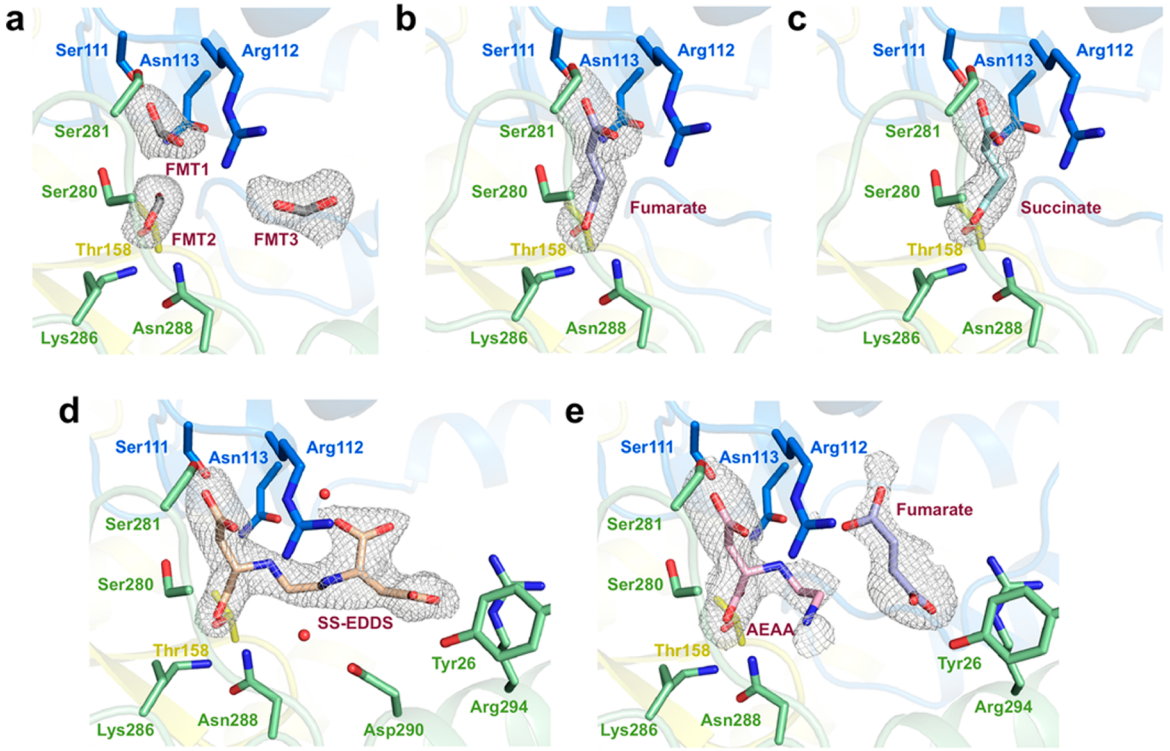

Figure 4. (a) Formate, (b) fumarate, (c) succinate, (d) (*S*,*S*)-EDDS, and (e) AEAA bound in the active site of EDDS lyase. The residues interacting with the ligands are shown as sticks in different colors (same coloring scheme as in Figure 2b). The gray mesh, contoured at 3σ, shows the simulated annealing $mF_o - DF_c$ omit map.

Interestingly, however, extra wedge-shaped electron density clearly indicated the presence of three formate ions bound in the active site (Figure 4a and Figure S4a). One formate ion (FMT1) makes hydrogen bonds to Ser111 and Arg112 (C1 region) from subunit A and Ser281 (SS loop) from subunit C, while another formate ion (FMT2) makes hydrogen bonds to Asn113 (C1 region) from subunit A, Thr158 (C2 region) from subunit B, and Lys286 and Asn288 (SS loop) from subunit C. The third formate ion (FMT3) is bound farther from the SS loop making an interaction with Arg112. On the basis of a comparison with other aspartase/fumarase superfamily structures, it was realized that two of these formate ions (FMT1 and FMT2) likely mimic the carboxylate groups of the succinyl moiety of the substrate, or of the product fumarate, when bound to the active site. To investigate this further, we repeated the crystallization experiments using solutions in which sodium formate was substituted with sodium salts of fumaric acid or succinic acid. Large cube-shaped crystals appeared overnight under conditions including a 0.2−0.3 M concentration of either salt, allowing the structural determination of fumarate-bound and succinate-bound EDDS lyase at 2.2 and 2.6 Å resolution, respectively (Table S2, Figure 4b,c, and Figure S4b,c). The fumarate and succinate molecules are tightly coordinated at the active site with overall identical binding interactions. As expected, the C1 and C4 carboxylate groups of fumarate/succinate occupy the same positions as formate ions FMT1 and FMT2 discussed above, making similar hydrogen bonds with residues from the C1, C2, and SS loop region. Most notably, the hydroxyl group of Ser280 in the SS loop (subunit C) is positioned close to (~3 Å) and in a proper orientation from the Cβ atom in fumarate/succinate, in accordance with its presumed role as a catalytic base in the α,β-elimination reaction.

EDDS- and AEAA-Bound Structures. Using an approach similar to that described above, crystals diffracting to 2.2 Å resolution were obtained of EDDS lyase grown in the presence of 0.3 M (*S*,*S*)-EDDS. Because the enzyme can convert (*S*,*S*)-EDDS to fumarate and ethylenediamine, we expected to observe a fumarate ion bound at the active site. Much to our surprise, however, the electron density at the active site was consistent with the presence of an intact (*S*,*S*)-EDDS molecule, allowing the determination of the substrate-bound structure (Table S2 and Figures 4d and 5). Apparently, the conditions for cleavage of (*S*,*S*)-EDDS in the crystal are not ideal, which may be explained by the non-optimal pH (6.5) of the crystallization solution (optimal pH for activity is 8) and/or insufficient protein flexibility preventing the deamination step and effectively trapping (*S*,*S*)-EDDS in the active site. One of the two succinyl moieties of (*S*,*S*)-EDDS (we refer to it as the proximal succinyl, on the basis of its proximity to the SS loop) binds at the active site like fumarate or succinate does in the other EDDS lyase structures, making identical interactions with the C1 and C2 regions and the SS loop (Figure 6). The other (distal) succinyl moiety points away from the active site and is bound near the protein surface, with one of the carboxylate groups forming hydrogen bonds with residues Arg294 and Tyr26 from chain C of the functional tetramer. The other largely solvent exposed carboxylate group makes a water-mediated hydrogen bond with Asn113. A comparison of the formate- and EDDS-bound structures shows that although the third formate ion (FMT3) and the carboxylate group of the distal succinyl moiety bind at similar regions of the active site pocket, their actual binding site locations and geometries are quite different (see Figure 4a,d). Thus, unlike FMT1 and FMT2, FMT3 indeed does not mimic the binding of one of the carboxylates of (*S*,*S*)-EDDS. In addition, the internal amino

DOI: 10.1021/acs.biochem.8b00406
Biochemistry 2018, 57, 3752−3763

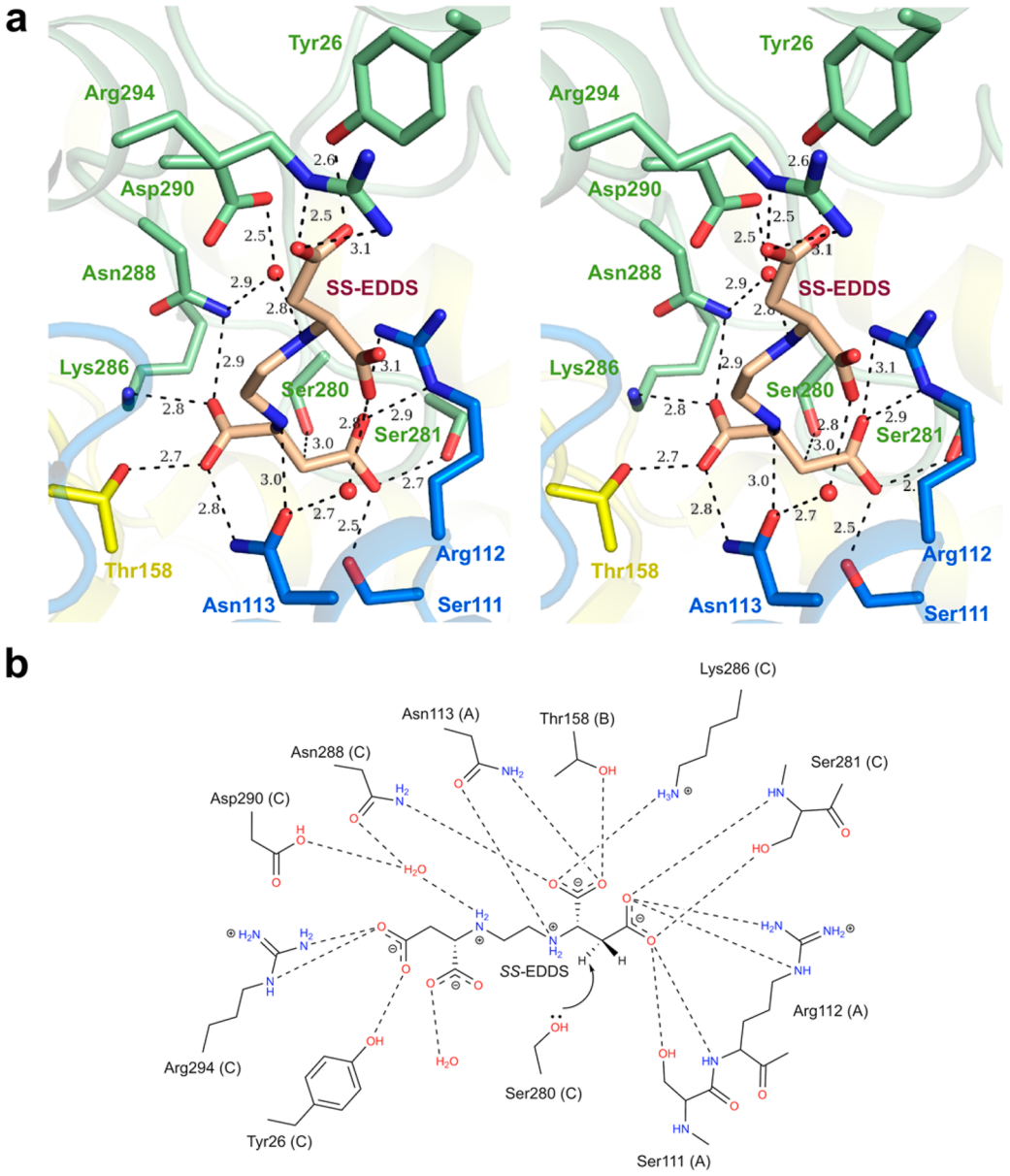

Figure 5. (a) Stereoview of the interactions of bound (*S*,*S*)-EDDS in the active site. Dashed lines show the hydrogen bonding interactions, and the labels show the distances in angstroms. (b) Schematic representation of the interactions between (*S*,*S*)-EDDS and active site residues. Hydrogen bonds are represented as dashed lines, and letters in parentheses denote the polypeptide chain identifier. The putative role of Ser280 as a catalytic base, abstracting the proton from the Cβ atom of (*S*,*S*)-EDDS, is shown with an arrow.

group of (*S*,*S*)-EDDS that is directly linked to the proximal succinyl moiety forms a hydrogen bond with Asn113, while the other amino group linked to the distal succinyl moiety makes water-mediated hydrogen bonds to Asn288 and Asp290.

To obtain a full description of all relevant structures in the catalytic cycle of EDDS lyase, crystals were also grown in the presence of the reaction intermediate AEAA. Surprisingly, instead of AEAA, a molecule of (*S*,*S*)-EDDS was found in the active site bound in an identical conformation as in the structure obtained from a crystal grown in the presence of (*S*,*S*)-EDDS (data not shown). A possible explanation for this result is that EDDS lyase in solution will reversibly cleave AEAA to fumarate and ethylenediamine. EDDS lyase likely first crystallizes in a fumarate-bound state, after which (*S*,*S*)-EDDS can be produced in the crystal in one step by attack of AEAA. This can happen as long as the concentration of AEAA in the crystallization solution is sufficiently high. Upon formation of (*S*,*S*)-EDDS in the crystal, it will remain trapped in the active site [as shown by the co-crystallization with (*S*,*S*)-EDDS]. In another attempt to obtain an AEAA-bound structure, a fumarate-bound crystal (prepared by crystallizing the enzyme in the presence of 0.3 M fumarate) was briefly soaked for ~30 s in mother liquor containing 20 mM ethylenediamine. The crystal was then immediately flash-cooled in liquid nitrogen and used for X-ray diffraction data collection. Difference Fourier analysis of the active site revealed a small adduct at the Cα atom of bound fumarate, most likely resulting from the addition of ethylenediamine to form the intermediate AEAA. Subsequent refinement yielded an AEAA-bound structure at 2.4 Å resolution (Table S2, Figure 4e, and Figure S4d). It should be noted that in this structure the ethylenediamine moiety of the bound AEAA molecule is relatively disordered, as indicated by

DOI: 10.1021/acs.biochem.8b00406
Biochemistry 2018, 57, 3752−3763

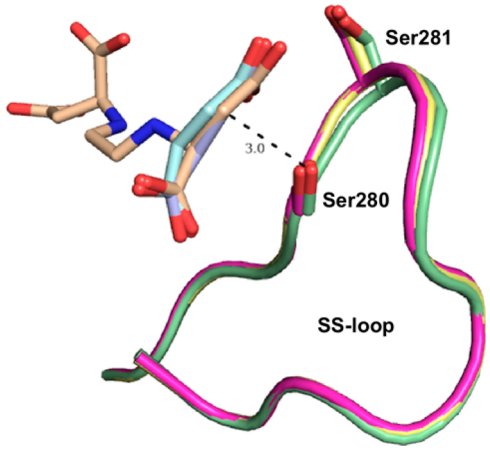

Figure 6. Superposition of bound (*S*,*S*)-EDDS (wheat), fumarate (light blue), and succinate (pale cyan) in the active site of EDDS lyase. The SS loops of the (*S*,*S*)-EDDS-bound, fumarate-bound, and succinate-bound structures, with putative catalytic base Ser280, are colored green, yellow, and magenta, respectively. The distance in angstroms from the hydroxyl group of Ser280 to the Cβ atom of the (*S*,*S*)-EDDS substrate is shown as a dashed line.

the absence of electron density for the terminal, free amino group. In addition, a second molecule of fumarate is observed near AEAA, bound at a location similar to where the distal succinyl moiety of (*S*,*S*)-EDDS binds. Possibly, this second molecule of fumarate prevented a quick release of AEAA, thereby inhibiting the full conversion toward (*S*,*S*)-EDDS.

Mutagenesis of Active Site Residues. The crystal structure of the enzyme in complex with (*S*,*S*)-EDDS (Figure 5) suggests important roles for Ser280 and Asp290 in catalysis and substrate binding, respectively. Ser280 is positioned near the Cβ proton of the substrate and in a suitable orientation to allow proton abstraction to initiate the deamination reaction. Asp290 forms a water-mediated hydrogen bond with the internal amino group connected to the distal succinyl moiety of (*S*,*S*)-EDDS, which appears to be an important interaction for binding and positioning of ethylenediamine for addition to fumarate. To study the importance of these residues for catalytic activity, each residue was replaced with an alanine. The mutation of Ser280 to an alanine resulted in an inactive enzyme (data not shown), confirming the essential role of this residue in catalysis. The mutation of Asp290 to an alanine resulted in a mutant enzyme that displayed activity significantly lower than that of wild-type EDDS lyase for the addition of ethylenediamine to fumarate (Figure S5).

DISCUSSION

The crystal structures of EDDS lyase determined in this study confirm a tertiary and quaternary fold that is characteristic of the aspartase/fumarase superfamily and provide the first detailed view of the substrate- and product-bound active site of an EDDS lyase, allowing an understanding of the roles of the various active site residues in substrate binding and catalysis (Figure 7). In all members of the aspartase/fumarase superfamily, a strictly conserved serine residue from the SS loop has been implicated to act as the catalytic base, abstracting a proton from the Cβ atom of the substrate to initiate the α,β-elimination reaction.[12,34−37] In EDDS lyase, the equivalent SS loop serine residue, Ser280, most likely functions as the catalytic base. Indeed, in both the (*S*,*S*)-EDDS-bound and the

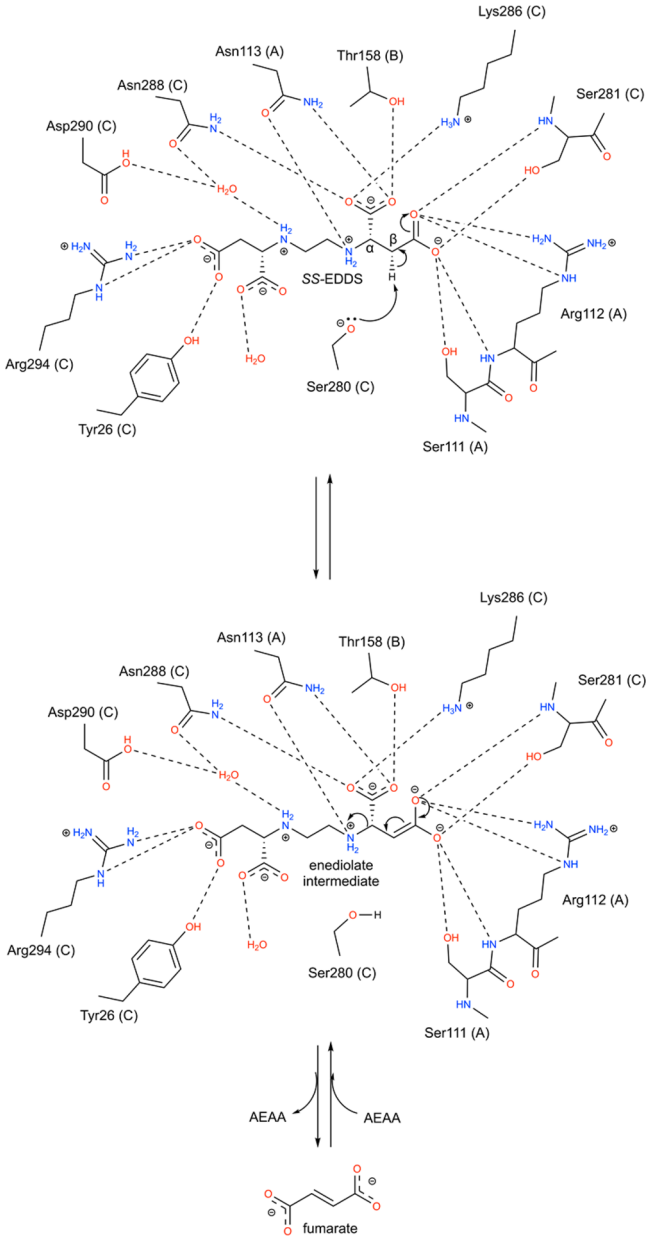

Figure 7. Proposed catalytic mechanism for the deamination of (*S*,*S*)-EDDS to yield AEAA and fumarate.

AEAA-bound structures, Ser280 is positioned near (~3 Å) the Cβ proton of the substrate (Figures 5, 6 and S4d) and in a suitable orientation to allow proton abstraction in the first step of the reaction (Figure 7). As expected, mutation of Ser280 to an alanine resulted in an inactive enzyme. However, for Ser280 to function as the catalytic base, it needs to be activated to form a Ser-O$^-$ oxyanion. Possible mechanisms for activation of the catalytic serine in aspartase/fumarase superfamily members have been suggested previously, including substrate-assisted deprotonation of the serine residue to generate the Ser-O$^-$ oxyanion.[12] The serine oxyanion could be stabilized by main chain amide interactions. In the structure of EDDS lyase, Ser280 is within hydrogen bonding distance of the neighboring main chain backbone amides of Ser281, Ile282, and Met283, which form part of the SS loop. The question of how Ser280 is activated to function as the catalytic base thus remains to be answered.

DOI: 10.1021/acs.biochem.8b00406
Biochemistry 2018, 57, 3752−3763

The extensive number of hydrogen bonding interactions observed for the binding of (*S*,*S*)-EDDS and AEAA (Figures 5 and S4d) forces the substrates to adopt an energetically unfavorable rotamer conformation in which the Cα, Cβ, and β-carboxylic atoms are coplanar. This is consistent with a conformation resembling a putative enediolate (*aci*-carboxylate) intermediate during catalysis (Figure 7).[12,36] The oxygens of the β-carboxylate group of (*S*,*S*)-EDDS and AEAA form hydrogen bonds with the side chain hydroxyls of Ser111 (subunit A) and Ser281 (subunit C, SS loop), the guanidinium moiety of Arg112 (subunit A), and main chain amides of Arg112 and Ser281. This extensive hydrogen bonding network not only is essential for substrate binding but also plays a crucial role in stabilizing the additional negative charge that develops on one of the β-carboxylate oxygens as a result of Cβ proton abstraction by Ser280. The presence of a positively charged residue, Arg112, has an additional stabilizing effect on the negatively charged *aci*-carboxylate intermediate. Both (*S*,*S*)-EDDS and AEAA are expected to employ similar catalytic mechanisms for the cleavage of the C−N bond (Figure 7). Hence, our results, combined with earlier mechanistic studies of other superfamily members,[12,34−37] support a mechanism that involves general base-catalyzed formation of a highly stabilized enediolate (or *aci*-carboxylate) intermediate during the sequential two-step deamination of (*S*,*S*)-EDDS.

The water-mediated hydrogen bond between Asp290 and the internal amino group connected to the distal succinyl moiety of (*S*,*S*)-EDDS (Figure 5) appears to be an important interaction for binding and positioning of ethylenediamine (and other diamine substrates) for addition to fumarate. Indeed, EDDS lyase seems to display higher amination activity using diamines as substrates than using monoamines (Table 1). The results showed that mutation of Asp290 to an alanine resulted in significant loss of activity of EDDS lyase for the addition of ethylenediamine to fumarate (Figure S5).

The crystal structures may also provide a possible explanation for the very broad substrate scope of EDDS lyase, which accepts a wide variety of amines (Table 1) and amino acids with terminal amino groups[14] for selective addition to fumarate. In the structures of most members of the aspartase/fumarase superfamily, the SS loop is intrinsically flexible and undergoes an open−closed transition upon binding of substrate.[12,34−37] This substrate-dependent movement of the SS loop is crucial because it positions catalytic and substrate-binding residues in a suitable orientation for catalysis and is accompanied by a closure of the active site pocket. Hence, the rather narrow substrate range of members of this superfamily may mirror this complex step in the catalytic mechanism. In EDDS lyase, however, the occurrence of an open−closed transition of the SS loop is highly unlikely; additional interactions with the N-terminal loop region stabilize a conformation of the SS loop that is highly similar to the catalytically competent closed conformation observed in the structures of other superfamily members, even when no substrate is bound. Thus, in contrast to superfamily lyases in which substrate-dependent movement of the SS loop positions catalytic and substrate-binding residues in a suitable orientation for catalysis and results in closure of the active site pocket, EDDS lyase appears to have a fully competent catalytic machinery in the uncomplexed enzyme, its SS loop does not seem to undergo conformational changes upon substrate binding, its active site pocket remains more accessible, and the pocket for the amine substituent is less defined. It is tempting to speculate that these unique structural properties reflect its very broad amine substrate scope and make EDDS lyase a more promising template for redesign to convert new unnatural substrates.

The crystal structures of EDDS lyase in complex with AEAA and (*S*,*S*)-EDDS set the stage for structure-based engineering of this fascinating enzyme. Improved variants of EDDS lyase with enhanced catalytic activity and an expanded unnatural substrate scope will provide a powerful synthetic tool for the preparation of diverse complex molecules by C−N bond formation. We have therefore initiated studies aimed at engineering of EDDS lyase, guided by the crystal structures reported here, to increase its synthetic usefulness in the production of metal-chelating aminocarboxylic acids as potential metallo-β-lactamase inhibitors, amino acid precursors for artificial dipeptide sweeteners, and substituted aspartic acids as aspartate/glutamate transporter inhibitors. The results of these studies will be reported in due course.

■ ASSOCIATED CONTENT

Supporting Information

The Supporting Information is available free of charge on the ACS Publications website at DOI: 10.1021/acs.biochem.8b00406.

Additional scheme, figures, and tables (PDF)

■ AUTHOR INFORMATION

Corresponding Authors

*E-mail: g.j.poelarends@rug.nl. Telephone: +31-50-3633354. Fax: +31-50-3633000.

*E-mail: a.m.w.h.thunnissen@rug.nl. Telephone: +31-50-3634380. Fax: +31-50-3634165.

ORCID

Gerrit J. Poelarends: 0000-0002-6917-6368

Present Addresses

§H.P.: Manchester Institute of Biotechnology, University of Manchester, 131 Princess St., Manchester M1 7DN, U.K.

∥J.d.V.: Strait Access Technologies, UCT Medical Campus, Anzio Road Observatory 7925, Cape Town, South Africa.

⊥V.P.V.: Reliance Technology Group, Reliance Industries Ltd., Navi Mumbai, India.

#H.R.: Chr Hansen, Bøge Alle 10-12, 2970 Hørsholm, Denmark.

Author Contributions

H.P. and J.d.V. contributed equally to this work.

Funding

This research was financially supported by ECHO Grant 700.59.042 from the Division of Chemical Sciences of The Netherlands Organisation of Scientific Research, the European Union seventh framework project Metaexplore (KBBE-2007-3-3-05, Grant Agreement 222625), and the European Research Council under the European Community's Seventh Framework Programme (FP7/2007−2013)/ERC Grant Agreement 242293. J.Z. acknowledges funding from the China Scholarship Council.

Notes

The authors declare no competing financial interest.

■ ACKNOWLEDGMENTS

The authors thank Marianne de Villiers, Haigen Fu, and Niels van Oosterwijk for insightful discussions and Marijke Jansma

DOI: 10.1021/acs.biochem.8b00406
Biochemistry 2018, 57, 3752−3763

for assistance with enzyme purification and crystallization. The authors also thank Johan Hekelaar for his assistance with data collection using an in-house X-ray generator.

REFERENCES

(1) Bucheli-Witschel, M., and Egli, T. (2001) Environmental fate and microbial degradation of aminopolycarboxylic acids. *FEMS Microbiol. Rev. 25*, 69−106.
(2) Oviedo, C., and Rodriguez, J. (2003) EDTA: The chelating agent under environmental scrutiny. *Quim. Nova 26*, 901−905.
(3) Madsen, E. L., and Alexander, M. (1985) Effects of chemical speciation on the mineralization of organic compounds by microorganisms. *Appl. Environ. Microbiol. 50*, 342−349.
(4) Allard, A.-S., Renberg, L., and Neilson, A. H. (1996) Absence of $^{14}CO_2$ from ^{14}C-labelled EDTA and DTPA and the sediment/water partition ratio. *Chemosphere 33*, 577−583.
(5) Nörtemann, B. (1999) Biodegradation of EDTA. *Appl. Microbiol. Biotechnol. 51*, 751−759.
(6) Nishikiori, T., Okuyama, A., Naganawa, T., Takita, T., Hamada, M., Takeuchi, T., Aoyagi, T., and Umezawa, H. (1984) Production by actinomycetes of (S,S)-N,N'-ethylenediaminedisuccinic acid, an inhibitor of phospholipase. *J. Antibiot. 37*, 426−427.
(7) Spohn, M., Wohlleben, W., and Stegmann, E. (2016) Elucidation of the zinc-dependent regulation in *Amycolatopsis japonicum* enabled the identification of the ethylenediamine-disuccinate ([S,S]-EDDS) genes. *Environ. Microbiol. 18*, 1249−1263.
(8) Witschel, M., and Egli, T. (1998) Purification and characterization of a lyase from the EDTA-degrading bacterial strain DSM 9103 that catalyzes the splitting of [S, S]- ethylenediaminedisuccinate, a structural isomer of EDTA. *Biodegradation 8*, 419−428.
(9) Egli, T. (2001) Biodegradation of metal-complexing aminopolycarboxylic acids. *J. Biosci. Bioengi. 92*, 89−97.
(10) Schowanek, D., Feijtel, T. C. J., Perkins, C. M., Hartman, F. A., Federle, T. W., and Larson, R. J. (1997) Biodegradation of [S, S], [R, R] and mixed stereoisomers of ethylenediamine disuccinic acid (EDDS), a transition metal chelator. *Chemosphere 34*, 2375−2391.
(11) Mizunashi, W. (2001) Protein having ethylenediamine-N,N′-disuccinic acid: Ethylenediamine lyase acitivity and gene encoding the same. U.S. Patent 6,168,940 B1.
(12) Puthan Veetil, V., Fibriansah, G., Raj, H., Thunnissen, A.-M. W. H., and Poelarends, G. J. (2012) Aspartase/fumarase superfamily: A common catalytic strategy involving general base-catalyzed formation of a highly stabilized aci-carboxylate intermediate. *Biochemistry 51*, 4237−4243.
(13) Nörtemann, B. (1992) Total degradation of EDTA by mixed cultures and a bacterial isolate. *Appl. Environ. Microbiol. 58*, 671−676.
(14) Fu, H., Zhang, J., Saifuddin, M., Cruiming, G., Tepper, P. G., and Poelarends, G. J. (2018) Chemoenzymatic asymmetric synthesis of the metallo-beta-lactamase inhibitor aspergillomarasmine A and related aminocarboxylic acids. *Nat. Catal. 1*, 186−191.
(15) Waddell, W. J. (1956) *J. Lab. Clin. Med. 48*, 311−314.
(16) Raj, H., Szymański, W., de Villiers, J., Rozeboom, H. J., Veetil, V. P., Reis, C. R., de Villiers, M., Dekker, F. J., de Wildeman, S., Quax, W. J., Thunnissen, A.-M. W. H., Feringa, B. L., Janssen, D. B., and Poelarends, G. J. (2012) Engineering methylaspartate ammonia lyase for the asymmetric synthesis of unnatural amino acids. *Nat. Chem. 4*, 478−484.
(17) Evans, P. R. (2006) Scaling and assessment of data quality. *Acta Crystallogr., Sect. D: Biol. Crystallogr. 62*, 72−82.
(18) Evans, P. R., and Murshudov, G. N. (2013) How good are my data and what is the resolution? *Acta Crystallogr., Sect. D: Biol. Crystallogr. 69*, 1204−1214.
(19) Collaborative Computational project, Number 4 (1994) The CCP4 suite: programs for protein crystallography. *Acta Crystallogr., Sect. D: Biol. Crystallogr. 50*, 760−763.
(20) McCoy, A. J., Grosse-Kunstleve, R. W., Adams, P. D., Winn, M. D., Storoni, L. C., and Read, R. J. (2007) Phaser crystallographic software. *J. Appl. Crystallogr. 40*, 658−674.
(21) Jaroszewski, L., Rychlewski, L., Li, Z., Li, W., and Godzik, A. (2005) FFAS03: server for profile-profile sequence alignments. *Nucleic Acids Res. 33*, W284−288.
(22) Sampaleanu, L. M., Codding, P. W., Lobsanov, Y. D., Tsai, M., Smith, G. D., Horvatin, C., and Howell, P. L. (2004) Structural studies of duck delta2 Crystallin mutants provide insight into the role of Thr161 and the 280s loop in catalysis. *Biochem. J. 384*, 437−447.
(23) Tsai, M., Sampaleanu, L. M., Greene, C., Creagh, L., Haynes, C., and Howell, P. L. (2004) A duck delta1 Crystallin double loop mutant provides insight into residues important for argininosuccinate lyase activity. *Biochemistry 43*, 11672−11682.
(24) Langer, G., Cohen, S. X., Lamzin, V. S., and Perrakis, A. (2008) Automated macromolecular model building or X-ray crystallography using ARP/wARP version 7. *Nat. Protoc. 3*, 1171−1179.
(25) Murshudov, G. N., Vagin, A. A., and Dodson, E. J. (1997) Refinement of macromolecular structures by the maximum-likelihood method. *Acta Crystallogr., Sect. D: Biol. Crystallogr. 53*, 240−255.
(26) Emsley, P., Lohkamp, B., Scott, W. G., and Cowtan, K. (2010) Features and development of Coot. *Acta Crystallogr., Sect. D: Biol. Crystallogr. 66*, 486−501.
(27) Adams, P. D., Afonine, P. V., Bunkoczi, G., Chen, V. B., Davis, I. W., Echols, N., Headd, J. J., Hung, L. W., Kapral, G. J., Grosse-Kunstleve, R. W., McCoy, A. J., Moriarty, N. W., Oeffner, R., Read, R. J., Richardson, D. C., Richardson, J. S., Terwilliger, T. C., and Zwart, P. H. (2010) PHENIX: a comprehensive Python-based system for macromolecular structure solution. *Acta Crystallogr., Sect. D: Biol. Crystallogr. 66*, 213−221.
(28) Schüttelkopf, A. W., and van Aalten, D. M. F. (2004) PRODRG: a tool for high-throughput crystallography of protein-ligand complexes. *Acta Crystallogr., Sect. D: Biol. Crystallogr. 60*, 1355−1363.
(29) Chen, V. B., Arendall, W. B., Headd, J. J., 3rd, Keedy, D. A., Immormino, R. M., Kapral, G. J., Murray, L. W., Richardson, J. S., and Richardson, D. C. (2010) MolProbity: all-atom structure validation for macromolecular crystallography. *Acta Crystallogr., Sect. D: Biol. Crystallogr. 66*, 12−21.
(30) Notredame, C., Higgins, D. G., and Heringa, J. (2000) T-Coffee: A novel method for fast and accurate multiple sequence alignment. *J. Mol. Biol. 302*, 205−217.
(31) Robert, X., and Gouet, P. (2014) Deciphering key features in protein structures with the new ENDscript server. *Nucleic Acids Res. 42* (W1), W320−W324.
(32) Krissinel, E., and Henrick, K. (2004) Secondary-structure matching (SSM), a new tool for fast protein structure alignment in three dimensions. *Acta Crystallogr., Sect. D: Biol. Crystallogr. 60*, 2256−2268.
(33) *PyMOL molecular graphics system*, version 1.6, Schrodinger, LLC.
(34) Sampaleanu, L. M., Vallee, F., Slingsby, C., and Howell, P. L. (2001) Structural studies of delta 1 and delta 2 Crystallin suggest conformational changes occur during catalysis. *Biochemistry 40*, 2732−2742.
(35) Tsai, M., Koo, J., Yip, P., Colman, R. F., Segall, M. L., and Howell, P. L. (2007) Substrate and product complexes of *Escherichia coli* adenylosuccinate lyase provide new insights into the enzymatic mechanism. *J. Mol. Biol. 370*, 541−554.
(36) Fibriansah, G., Puthan Veetil, V., Poelarends, G. J., and Thunnissen, A.-M. W. H. (2011) Structural basis for the catalytic mechanism of aspartate ammonia lyase. *Biochemistry 50*, 6053−6062.
(37) Mechaly, A. E., Haouz, A., Miras, I., Barilone, N., Weber, P., Shepard, W., Alzari, P. M., and Bellinzoni, M. (2012) Conformational changes upon ligand binding in the essential class II fumarase Rv1098c from *Mycobacterium tuberculosis*. *FEBS Lett. 586*, 1606−1611.

DOI: 10.1021/acs.biochem.8b00406
Biochemistry 2018, 57, 3752−3763